

Using SU-8 with a viscosity of 7.5 cSt, the barrier height and the translation stage speed determine the coating thickness which, in turn, determines the stimulated emission wavelength of the DFB laser. The relationship between the film thickness and the translation speed was studied using an atomic force microscope (AFM) (Digital Instruments Dimension 3000 Atomic Force Microscope, Veeco) and an optical interferometry profiler (Veeco NT1000 optical profiler, Veeco). In addition, since the thickness of the gain layer is closely related to the stimulated emission wavelength, by measuring the laser emission spectrum as a function of the spatial location, we can also map out the spatial variation of the refractive index of the laser surface, so as to characterize the uniformity or surface morphology of the device.

2.3 Active layer pattern process

For some applications, it is useful to have a patterned device, in which selected regions of the surface are not capable of lasing action. Using SU-8 as the laser dye host allows us to easily pattern the light emission area in any shape using the conventional photolithography. As mentioned above, after the device was soft baked on a 95 °C hotplate for 1 min to remove the solvent, the device was photopolymerized by exposure to UV radiation ($\lambda = 365$ nm lamp source) through a photomask. To demonstrate this, we designed a photomask with the pattern of a Chinese character “中” which occupies a 1mm \times 1mm area with a feature size of 125 μ m. The exposed film was post-baked at 95 °C for 120 seconds and the unexposed area was removed by the developing process, resulting in a patterned area with a negative image of the pattern mask.

Previous work has shown that the nanoreplica molding process is capable of reproducing sub-wavelength grating structures over large surface areas [4], and implementation of a roll-to-roll process for high volume manufacturing [37]. We envision that the horizontal dipping process can be implemented as a process that can be performed in a roll-to-roll manner upon replica-molded grating structures either on a separate piece of manufacturing equipment, or integrated within a machine that can perform both processes.

3. Test instrumentation

Figure 3 shows a schematic diagram of the experimental setup used to characterize the performance of the fabricated DFB laser. Optical pumping was provided by a frequency-doubled, Q -switched Nd: YAG pulse laser ($\lambda_p = 532$ nm, yttrium aluminum garnet) with a pulse duration of 10ps at a maximum repetition rate of 10 Hz. The pumping beam passed through a spatial filter and a 10 \times beam expander and a spatial filter to spatially clean the beam. Focused by a 10 \times objective, the pumping beam formed a ~ 4 μ m diameter spot on the DFB laser surface which was placed on the focal plane of the objective.

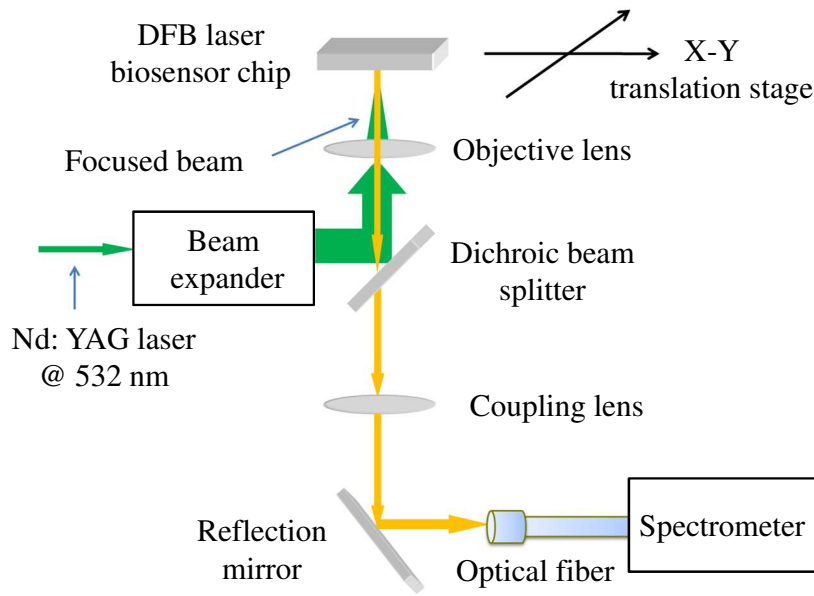


Fig. 3. Schematic diagram of the DFB laser detection instrumentation setup.

The lasing emission from the device was collected by the same objective and then passed through a dichroic mirror and a long pass emission filter that eliminated the strong pumping light. Because a 1D DFB resonator only provides confinement perpendicular to grating axis, the beam is highly divergent along the direction parallel to the grating axis [44,45]. To account for this effect, the stimulated emission was coupled into a step index multimode fiber ($d = 600 \mu\text{m}$, $\text{NA} = 0.48$) with a large numerical aperture (NA) using a convex lens. Finally, a spectrometer (iHR550, Horiba Jobin Yvon) with a 1800 lines/mm grating and a charge coupled device was used to analyze the emission spectrum. The measured laser emission was fitted with a Lorentzian distribution model to precisely determine the peak wavelength value (PWV).

4. Device characterization

4.1 Film thickness

For the horizontal dipping process, the coating polymer is categorized as a Newtonian liquid which is usually characterized by its viscosity, density, and surface tension. A downstream meniscus shape will form after the solution is fed into the gap between the stainless steel barrier and the grating surface. The relationship between the film thickness and the radius of the curvature of the downstream meniscus is given by Eq. (1):

$$t_w = 1.34 \left(\frac{\mu U}{\sigma} \right)^{2/3} \cdot R_d. \quad (1)$$

where R_d represents the radius of curvature of the downstream meniscus, μ and σ represent the viscosity and surface tension of the coating solution, respectively, and U is the carrying speed [40]. During the coating process, the gap between the stainless steel barrier and the grating surface was kept at 0.9 mm and the translation velocity of the barrier was adjusted from 0.01 cm/s to 0.8 cm/s. The resulting gain layer thickness ranged from 234.0 nm to more than 3.1 μm , as shown in Fig. 4. With the lowest translation speed of 0.01 cm/s, a film thickness of ~234 nm was achieved. The film thickness is measured both by an atomic force microscope (AFM) (Digital Instruments Dimension 3000 Atomic Force Microscope, Veeco) and an

optical surface profiler (Veeco NT1000 optical profiler, Veeco). The measurement results are compared to the theoretical prediction, shown as the red curve in Fig. 4.

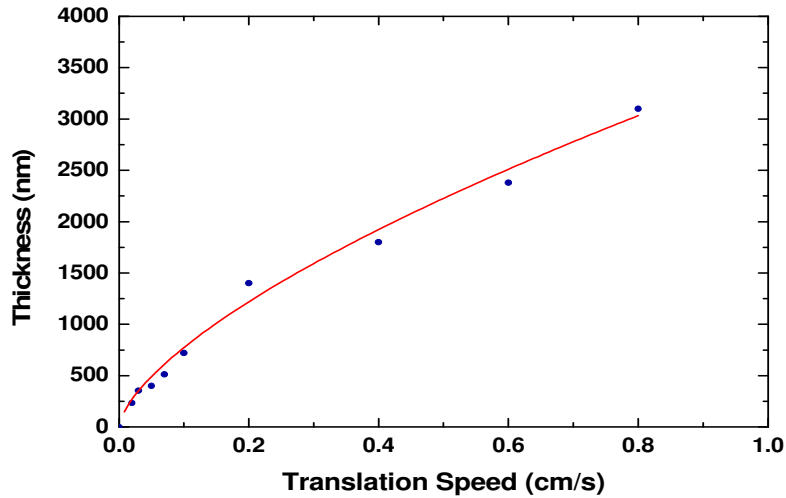


Fig. 4. Relationship between the translation speed of the carrier stage and the guidance layer thickness: the translation speed ranges from 0.01cm/s to 0.8cm/s and the corresponding film thickness ranges from 234nm to $\sim 3.1\mu\text{m}$.

4.2 DFB laser performance

Another advantage of this fabrication strategy is the wide tunability of the lasing emission wavelength. As mentioned in the device design section, the lasing wavelength could be tuned within the emission spectral region of the gain material by modifying the effective refractive index by controlling of the thickness of the wave guidance layer. The emission wavelengths of devices with different guidance layer thicknesses were measured, and are shown in Fig. 5. Since the guidance layer has a larger refractive index compared to the superstrate media and the substrate layer, an increase in the thickness of the guidance layer will introduce a red shift in the lasing emission wavelength. The relationship between the guidance layer thickness and the stimulated emission wavelength is depicted in the inset plot. Single mode emission was observed when the guidance layer thickness was within a range of 234-510 nm. When a much thicker guidance layer was employed, the laser began to emit multiple modes, as shown in the top left inset plot.

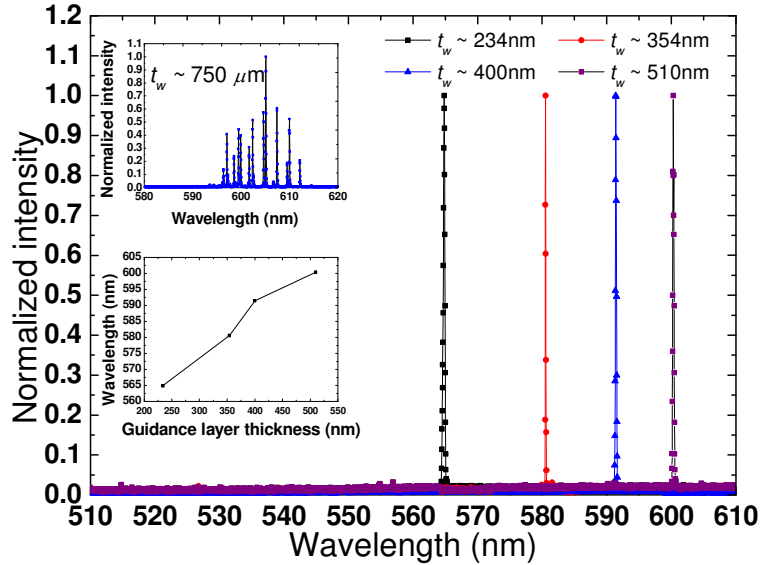


Fig. 5. Stimulated emission characteristics of devices with various guidance layer thicknesses (t_w). The fabricated lasers exhibit a linewidth of $\Delta\lambda = 0.15$ nm, threshold pump fluence ~ 0.169 mJ-cm $^{-2}$ at $\lambda = 532$ nm. The top left inset picture shows multiple modes emission when the guidance layer thickness is ~ 750 μ m. The bottom left inset plot shows the relationship between the laser emission wavelength and the guidance layer thickness.

4.3 Film thickness uniformity

Due to the relationship between the thickness of the guidance layer and the laser emission wavelength, the uniformity of the device can be investigated by measurement of the spatial distribution of stimulated emission wavelengths. The measurement results are shown in Fig. 6. The laser emission wavelength measurement was first performed in a line-by-line manner with 2mm spacing between adjacent sampling spots on a device having an area of 50mm \times 20mm, as shown in the top of Fig. 6. The range of the PWV variation is $\Delta\lambda \sim 3.15$ nm, which indicates a variation range of ~ 36 nm of the guidance layer thickness according to rigorous coupled wave analysis (RCWA) simulations of the device structure (simulation results not shown). The standard deviation of PWV is 0.514nm, resulting in a coefficient of variation of $CV = 0.087\%$. To characterize the uniformity with a finer spatial scale over a small surface area, a zoomed in measurement was performed in a single 2mm \times 2mm square, with 125 μ m spacing between adjacent sampling spots. As shown in the bottom of Fig. 6, the PWV range was $\Delta\lambda = 0.481$ nm, with a standard deviation of 0.129 nm and a coefficient of variation of $CV = 0.022\%$. The measured standard deviation of DFB output wavelength corresponds to only ~ 1.57 nm standard deviation of the guidance layer thickness over a 4 mm 2 area. These results were further verified by an AFM measurement.

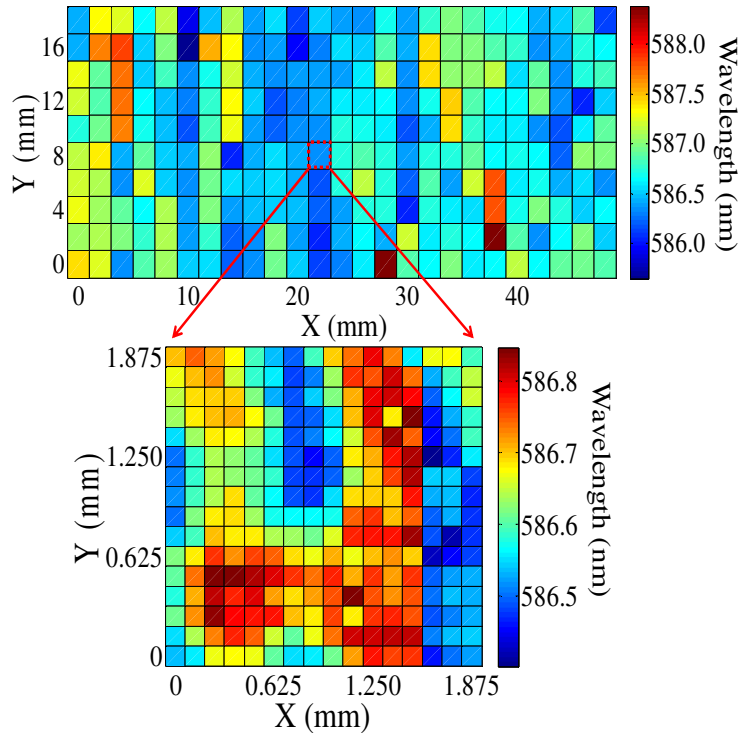


Fig. 6. Spatial distribution of the laser emission wavelength. The top picture illustrates a map of laser emission wavelength over a 5cm \times 2 cm area. For such an area, the laser emission varies within a range of 3.15nm. The bottom picture shows a zoomed-in perspective of the lasing wavelength distribution within a single grid with a 2mm \times 2 mm area, where the laser emission ranges from 586.41nm to 586.89nm.

4.4 Emission image of patterned DFB laser

In some applications, it is desirable for the laser light source to be patterned. For example, for our application for creating DFB laser biosensors, it is often desirable to create discrete regions of DFB laser surface that can be functionalized with different capture molecules for creating an array of small sensors that can be probed individually. Patterning by photolithography is an established fabrication process involving simple steps, including photoresist (PR) coating, PR baking, exposure, developing, material etching and PR stripping. Devices made by the method described in this work can be easily patterned using photolithography, while still in a roll-based format because the horizontal-dipped layer of the dye-doped SU-8 is photosensitive.

Figure 7 shows the spatial laser emission profile of a device with a patterned SU-8 layer, using the process described in Section 2.3, in which the mask was created by printing ink on a transparent plastic sheet with a laser printer. Since the laser-printed pattern has a feature resolution of 125 μm , the spatial resolution between the adjacent pumping spot was chosen to be 12.5 μm to satisfy the Nyquist sampling frequency. In Fig. 7, regions that do not lase are assigned a wavelength of 0 nm, and are displayed in black. The spatial distribution of the stimulated emission wavelength along the horizontal direction is also shown. The variation is within a $\Delta\lambda = 0.14$ nm range.

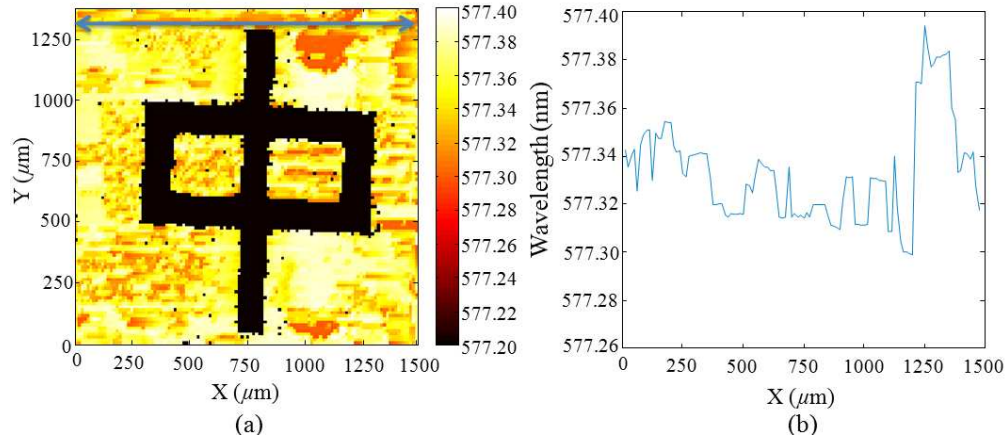


Fig. 7. Emission characteristics of a patterned DFB laser. (a) The stimulated emission image of a patterned DFB laser: The black part with a pattern “中” indicates the dumb region where the gain layer has been removed. So the laser does not lase there, while the laser works normally in the complementary region. The spatial resolution of the image is $12.5\mu\text{m}$, and the feature size of the pattern is $125\mu\text{m}$. (b) The spatial distribution of the stimulated emission wavelength cross a horizontal line in (a): The variation of the lasing emission cross the horizontal line is within a 0.14 nm range, while the lasing wavelength difference between adjacent spots is less than 0.01 nm .

5. Conclusion

A fabrication method that combines nanoreplica molding and horizontal dipping processes has been developed for organic DFB lasers upon flexible plastic substrates. The spatially corrugated surface can be produced inexpensively and in virtually any periodicity upon a plastic substrate by the nano-replica molding method. The subsequent horizontal dipping process allows uniform coating of dye doped polymer active layer onto the grating surface at desired thickness ranging from 234.0 nm to $3.1\mu\text{m}$. Lasing from the polymer-based DFB structure, having a replicated $\Lambda = 400\text{ nm}$ polymer grating and a Rhodamine 590 doped SU-8 active medium, has been demonstrated and characterized. The laser emission wavelength can be controlled in the $\lambda = 564.82\text{-}600.33\text{ nm}$ wavelength range. The tested DFB laser exhibits a linewidth of $\Delta\lambda = 0.15\text{ nm}$, a threshold pump fluence $\sim 0.169\text{ mJ}\cdot\text{cm}^{-2}$ at $\lambda = 532.00\text{ nm}$, and emission wavelength variations as small as 3.15 nm over a 10 cm^2 area. From this example of a plastic DFB laser, it is clear that the developed fabrication method has the capability of producing organic DFB laser and organic DFB laser arrays for a wide range of wavelengths.

Acknowledgement

This project was made possible by a cooperative agreement that was awarded and administered by the U.S. Army Medical Research & Materiel Command (USAMRMC) and the Telemedicine & Advanced Technology Research Center (TATRC), under Contract #: W81XWH0810701. The authors also extend their gratitude to the support staff of Micro and Nanotechnology Laboratory at University of Illinois at Urbana-Champaign.